This Publication Is Distributed To Members Only

Harmonics and Transients Tech Notes

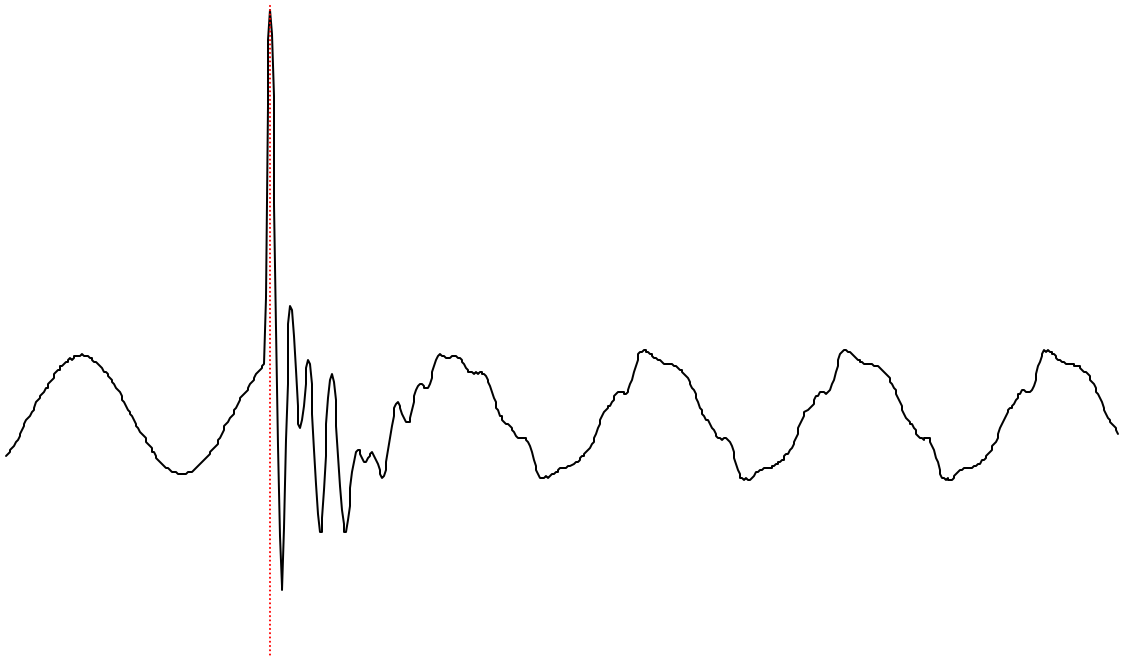

Issue # 99-2 ***June 1999*** ***Editor: Sandy Smith***

Project Manager: Tom Grebe

In this issue:

Letter from the Project Manager:

Dear PATH Members:

Welcome to another edition of *Tech Notes.* We hope you find this issue to be both informative and interesting. With one article on emtp computational methods and two articles touching on harmonics, this particular issue has something for everyone.

This thrice-yearly publication exists thanks to the contributions of our university members. In exchange for a no-cost membership, members must agree to submit a technical paper or presentation for distribution to the user group membership. While most of these papers end up in *Tech Notes*, contributions can take other forms. These include:

- Case studies or technical presentations for the Users Group annual meeting
- Modules and models for presentation and distribution at the annual workshop
- Modules and models developed for distribution on the Web site
- Library files developed for the Web site

Topics have a wide range. They can include:

- Applications/models for SuperHarm/HarmFlo+ and transient-modeling tools
- Case studies/unique simulations
- Research projects
- EMTP data preparation/model development
- SuperHarm/HarmFlo data preparation/filter design
- Technical issues dealing with harmonics or transients

In addition to encouraging material from university members, we accept contributions from other members as well. If you have a paper, presentation, model, etc., and would like to submit it, please let us know. Likewise, if you have a question or comment about the user group, we want to know about it as well. Feedback helps us to do better our job of running the users group.

As always, we appreciate your support of PATH.

Sincerely,

Thomas Grebe, P.E.
General Manager, Electrotek Consulting
PATH Users Group Project Manager

Computational Methods For EMTP Steady-State Initialization

Juan A. Martinez-Velasco
Departament d'Enginyeria Elèctrica
Universitat Politècnica de Catalunya
Barcelona - Spain

Abstract - The calculation of the non-sinusoidal periodic steady-state of a power system with nonlinear and variable-topology components becomes an important problem in the application of some electromagnetic transients programs. A dedicated procedure for obtaining the initial steady-state with harmonics is therefore an important feature. This paper presents a summary of the techniques used for emtp steady-state initialization. These techniques are classified into three groups: frequency-domain, time-domain, and hybrid methods. The advantages and limitations of each group are discussed.

Keywords : Transients Analysis, EMTP, Steady-State Initialization.

1. Introduction

The development of the first EMTP (ElectroMagnetic Transients Program) was undertaken in the late sixties to duplicate TNA transients simulations. Since then, the capabilities and applications of this tool have been significantly increased. In addition, other electromagnetic transients programs (emtps) based on the same solution method have been developed [1], [2]. One of the capabilities implemented in some transients programs is a steady-state initialization algorithm. The applications for which such an algorithm is a very useful feature are many, i.e.. subsynchronous resonance, harmonic propagation.

Several important aspects are to be considered in an initialization method for emtp usage :

- many nonlinear components (transformers, rotating machines, switched converters) generate harmonics
- in many applications (i.e. power electronics converters), control systems are included in the simulation, then the initialization of control systems should be also performed
- there are several emtp applications for which different initialization methods are needed, i.e., frequency scan analysis and load flow calculation
- different initial specifications must be dealt with; i.e., voltage and power constraints (load flow data)
- several types of waveshapes can result in an initial steady state : periodic at power frequency, periodic with harmonics, quasi- or non-periodic.

The development and implementation of a unique steady-state initialization procedure that can cover all emtp potential applications is a very difficult task. A very intense activity has been performed in the development of procedures for the initial steady-state calculation in networks with nonlinear and variable-topology converters during the last thirty years [3], [4], [5]. Many algorithms with a limited number of applications have been proposed for emtp initialization, and some have already been implemented.

This paper presents a summary of the most important procedures for emtp steady-state initialization of networks with nonlinear components. The study deals with the initialization of power systems and control strategies, and only the case of a periodic initial steady-state is considered. This paper includes a short introduction to emtp solution methods, and a discussion on the limitations of the procedures for emtp initialization.

2. EMTP solution methods

2.1 Transient solution of power networks

Electromagnetic transients programs are circuit-oriented tools based on a time-domain solution method, the Dommel's scheme. It combines the Bergeron's method and the trapezoidal rule into an algorithm capable of solving transients in single- and multi-phase networks with lumped and distributed parameters. The trapezoidal rule is used to convert the differential equations of the network components into algebraic equations involving voltages, currents and past values. These algebraic equations are assembled using a nodal approach [1]

$$\mathbf{[G]\,[v(t)] = [i(t)] - [I]} \qquad (1)$$

where **[G]** is the nodal conductance matrix, **[v(t)]** is the vector of node voltages, **[i(t)]** is the vector of current sources, and **[I]** is the vector of "history" terms.

When the network contains voltage sources to ground, the equation is split up into part A with unknown voltages and part B with known voltages

$$\mathbf{[G_{AA}]\,[v_A(t)] = [i_A(t)] - [I_A] - [G_{AB}]\,[v_B(t)]} \qquad (2)$$

The conductance matrix is symmetrical and remains unchanged as the integration is performed with a fixed time-step size. The solution of the transient process is then obtained using triangular factorization.

Several modifications have been proposed for solving networks nonlinear and time-varying elements [2], [6]. One of the most efficient is based on the compensation method. Nonlinear elements are represented as current injections which are superimposed to the solution of the linear network after this solution has been computed. Once the solution of the network without the nonlinear element has been computed, its contribution is deduced from the characteristic of the nonlinear element, $v_b(i_b(t))$, and the following equation

$$v_b = v_{b(0)} - r_{thev}\, i_b \qquad (3)$$

where $v_{b(0)}$ is the voltage solution without the nonlinear element, and r_{thev} the Thevenin equivalent resistance. An iterative solution, generally based on the Newton's method, must be used to solve this step. The compensation method can be generalized to networks with several nonlinear components. However, its application is limited to only one nonlinear element per node. Other solution methods has been proposed to solve this limitation [7].

Programs based on the trapezoidal rule are widely used for transient simulations due to the simplicity of this integration rule, as well as to its numerical stability. The trapezoidal rule is an A-stable method that does not produce run-off instability [2]. However, this rule has some drawbacks – it uses a fixed time-step size and can originate sustained numerical oscillations. The step size determines the maximum frequency that can be simulated; therefore users have to know in advance what is the frequency range of the transient simulation.

2.2 Numerical oscillations

In switching operations or transitions between segments in piecewise-linear inductances, the trapezoidal rule acts as a differentiator, and introduces sustained numerical oscillations. Several techniques have been proposed to control or reduce these numerical oscillations. One technique uses additional damping to force oscillations to decay [8]: the damping can be provided by the integration

rule itself or externally, by adding fictitious resistances in parallel with inductances and in series with capacitors. This method can have an important effect on the accuracy of the solution. Another technique is based on the use of snubber (RC) circuits in parallel with switches. This option is very interesting in power electronics applications, as snubber circuits are often placed in parallel with semiconductors to limit overvoltages across them.

Other techniques are based on the temporary modification of the solution method, only when numerical oscillations can occur, without affecting the rest of the simulation. These techniques use interpolation [9], or a CDA (Critical Damping Adjustment) procedure [10].

2.3 Transient solution of control systems

Control systems can be represented by block diagrams with interconnection between system elements. Control elements can be transfer functions, FORTRAN algebraic functions, logical expressions and some special devices [2], [11]. A linear block can be described in the s-domain by a general relationship X(s) = G(s) U(s), where U(s) and X(s) are respectively the input and the output, and G(s) is a rational transfer function. The solution method used in all transients programs is also based on the trapezoidal rule, being transfer functions converted into algebraic equations in the time-domain, with the following general form

$$[A_{xx}][x] + [A_{xu}][u] = [hist] \qquad (4)$$

These equations are by nature unsymmetrical. Due to this fact, the electric network and the control system are solved separately. The network solution is first advanced, the network variables are next passed to the control section, control equations are then solved. Finally, the network receives control commands. The whole procedure introduces a time-step delay. This procedure is simultaneous only for linear blocks, and sequential for nonlinear blocks. When these blocks are present, a true simultaneous solution is not performed. A closed-loop is broken and the system is solved by inserting a time delay.

Delays inside control loops, as well as the delay between the network and the control system, are sources of instabilities and inaccuracies. In addition, new applications have been demanding capabilities not available in the first versions, i.e., new digital controls. Work has been performed during the last years to overcome most limitations and minimize some problems [12], [13], [14].

3. Initialization methods

The solution of a transient phenomenon is dependent on the initial conditions with which the transient is started. Although some simulations can be performed with zero initial conditions, there are many cases for which the simulation must be started from power-frequency steady-state conditions. In addition, an initialization procedure can be a useful tool on its own, for instance to calculate resonant voltages due to coupling effects between parallel transmission lines.

The steady-state solution of linear networks at a single frequency is a simple task, and can be obtained using nodal admittance equations [2]

$$[Y][V] = [I] \qquad (5)$$

where **[Y]** is the nodal complex admittance matrix, **[V]** is the vector of node voltages, **[I]** is the vector of current sources. As for the transient solution, this equation is partitioned when the network contains voltage sources to ground.

$$[Y_{AA}][V_A] = [I_A] - [Y_{AB}][V_B] \qquad (6)$$

This task can be very complex in the presence of nonlinearities that can produce steady-state harmonics. The initial solution with harmonics can be obtained using some simple approaches. The simplest one is known as "brute force" approach: the simulation is started without performing any initial calculation and carried out long enough to let the transients settle down to steady-state conditions. This approach can have a very slow convergence if the network has components with light damping. A more efficient method is to perform an approximate linear ac steady-state solution with nonlinear branches disconnected or represented by linearized models. Some transients programs have a "snapshot" feature. Using a "brute force" initialization, the system is started from standstill, once it reaches the steady-state, a snapshot is taken and saved, so later runs can be started at this point.

One of the first methods, Initialization with Harmonics (IwH), was presented in [15]. It is an iterative procedure to obtain the magnitude of harmonics generated by saturable reactors. Here, nonlinear inductances are modeled as voltage-dependent harmonic current sources. The model of the power network is linear, therefore the voltages at any harmonic frequency can be found by solving the nodal equations. Other harmonic sources whose magnitude is known are included in the solution as additional current or voltage sources. The periodic steady-state solution is computed using two iterative loops:

a) A preliminary step is used to calculate the voltage phasors of nonlinear inductances taking into account their V_{RMS} - I_{RMS} characteristic.
b) These voltages are used to obtain the current harmonics from the actual flux-current characteristic. These harmonics are reinjected back into the network to calculate a new set of voltage phasors that are superposed to find the new fluxes.

The procedure continues with the calculation of the new harmonic currents until convergence is achieved. This is a very simple procedure. However, it can fail to converge and cannot be applied to ferroresonance studies [15], [19].

The initialization of control systems is an important issue in many emtp applications, i.e., power electronic systems. The first versions allowing users to represent control system dynamics did include a very simple and limited initialization algorithm [11], only applicable to linear systems. Several improvements have been added to some programs [12], but the initialization feature is still very limited.

Several computational methods for emtp initialization have been developed after IwH was presented. They can be classified into three groups : frequency-domain, time-domain, and hybrid methods. The procedure above described can be considered as a hybrid method as it mixes frequency-domain calculations using nodal admittance equations with a time-domain calculation for obtaining the values of the harmonic current sources used to represent nonlinear reactances. A summary of the most relevant methods proposed up to date, and presented after Iwh, is given in the subsequent sections.

3.1 Frequency-domain methods

These are the most efficient when the network has a linear behavior, and the natural approach when the initial operating conditions include power (load flow) constraints. Most procedures use one the two techniques summarized below.

a) Fixed-point iterative methods: At each iteration, the latest values of the distorted terminal voltages are used to drive updated information of the harmonic current injections. The nodal equations of the linear network are then invoked to update the voltage harmonics for the next iteration.
b) Newton-type methods: The equations of the linear and the nonlinear parts are solved simultaneously at any harmonic frequency.

Two approaches have been proposed to represent nonlinear components: a harmonic current source, and a Norton equivalent (NE). The two methods described below were developed as improvement of the IwH. Both use a NE to represent nonlinear components.

1 - Multiphase Harmonic Load Flow (MHLF) [16], [17]

A nonlinear component is represented by means of a Norton equivalent at each harmonic frequency. Although only Thyristor Controlled Reactor (TRC) applications were analyzed in the original references, the methodology can be extended to other nonlinear components. Fig. 1 shows the TCR equivalent model. The inductance at fundamental frequency is

$$L_{eq} = \pi L \left(\sigma - \sin\sigma\right)^{-1} \qquad (7)$$

where σ is the conduction angle. This inductance can also be used to represent the TCR at higher frequencies, therefore

$$Y_{eqh} = \left(jh\omega L_{eq}\right)^{-1} \qquad (8)$$

The value of the equivalent harmonic current source is derived from the calculated voltage and current harmonics using the following expression

$$I_{eqh} = (jh\omega L_{eq})^{-1} V_h - I_h \qquad (9)$$

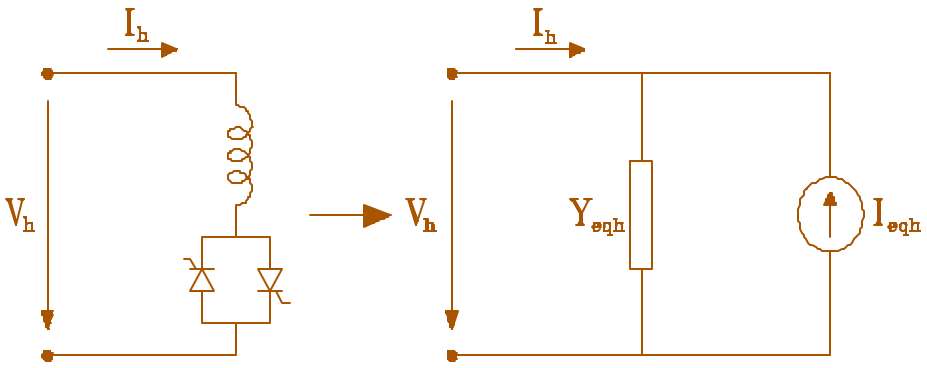

Fig. 1. Norton equivalent model for a TCR [16].

With this approach, the NE circuits are harmonically decoupled and the load flow solution is performed sequentially for one harmonic at a time. However, the coupling effects are included as the harmonic current sources are iteratively adjusted, see Discussion of [16].

The general procedure is based on a fixed-point iterative technique, as the IwH. In addition to an initialization stage, which is particularly important in load flow solutions of multiphase unbalanced networks, the procedure consists of two basic steps:

a) The solution of the network at the fundamental and the harmonic frequencies is solved using a Newton-Raphson method. The general form is expressed as

$$\mathbf{F([X]) = 0} \qquad (10)$$

where **[X]** is the vector of state variables.

b) The harmonic NE circuits of nonlinear components are derived, and convergence is checked by comparing I_{eqh} from two successive iterations.

The synchronous machine is a special component in power networks. This component may generate harmonics under unbalanced conditions, and the saturation effects can complicate its response to harmonics from other sources. A three-phase synchronous generator model for unbalanced harmonic load flow analysis, including frequency conversion and saturation effects, was presented in [18].

A simpler multiphase power flow solution based on the MHLF procedure was presented in [19].

2 - Newton harmonic method [20]

The Norton equivalent of a nonlinear branch at a harmonic frequency is derived as follows, see Fig. 2,

- the admittance G_{bo} is calculated at each iteration as the mean value of

$$\left.\frac{dg_b}{dv_b}\right|_{v_b^{(k)}} \tag{11}$$

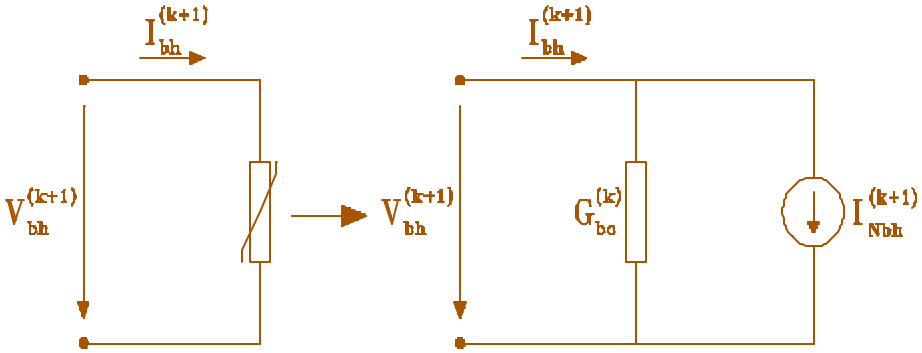

Fig. 2. Norton equivalent of a nonlinear branch [20].

- the current source value is then calculated using

$$I_{Nbh}^{(k+1)} = I_{bh}^{(k)} - G_{bo}^{(k)} V_{bh}^{(k)} \tag{12}$$

being I_{bh} the harmonic current source component found from v_b and the characteristic of the nonlinear branch.

This approach accounts for harmonic coupling, and is an exact solution. The equivalent circuits of nonlinear branches are included at each iteration in the nodal equations of the linear network. The general formulation for each harmonic *h* becomes

$$\mathbf{[Y_{nh}^{(k)}][V_{nh}^{(k+1)}] = [I_{nh}^{(k+1)}]} \tag{13}$$

where

$$\mathbf{[Y_{nh}^{(k)}] = [A][Y_h^{(k)}][A]^t} \tag{14}$$

$$\mathbf{[I_{nh}^{(k+1)}] = [A]\ ([I_{Sh}] - [I_{Nh}^{(k+1)}])} \tag{15}$$

being $\mathbf{[Y_{nh}]}$ the nodal admittance matrix and $\mathbf{[Y_h]}$ the branch admittance matrix. $\mathbf{[V_{nh}]}$ is the vector of node voltages, $\mathbf{[I_{nh}]}$ is the vector of injected currents, $\mathbf{[I_{Sh}]}$ is the vector of independent current sources, and $\mathbf{[I_{Nh}]}$ is the vector of equivalent current sources. **[A]** is the incidence matrix.

The procedure is initialized without nonlinear branches, unless an approximated model at fundamental frequency was available. After computing $\mathbf{[V_n]}$ at each harmonic frequency, the Norton equivalent of all nonlinear branches is determined, and $\mathbf{Y_{nh}}$ and $\mathbf{I_{nh}}$ are updated. The procedure is continued until

convergence. This is not a true Newton-Raphson method, as discussed in [20]. However, it shows a quadratic convergence and can be applied to ferroresonance cases.

Other frequency-domain methods were presented in [21] and [22].

3.2 Time-domain methods

Steady-state initialization algorithms based on a time-domain solution are formulated as a two-point boundary value problem, and use an iterative Newton type approach. If a solution of period T is assumed for all network variables, and **[X]** denotes the vector of state variables, an iterative procedure is set up to meet two general constraints at the steady state solution

- the periodicity condition

$$[X_0] = [X_T] \tag{16}$$

  being $[X_0]$ and $[X_T]$ the vectors of state variables at time 0 and T, respectively

- the relationship between the network solution at two different time steps, usually elapsed one period T,

$$[X_T] = F([X_0]) \qquad ([X_T] = [X(T, X_0)]) \tag{17}$$

A system of equations can be defined then as follows

$$H([X_0]) = F([X_0]) - [X_0] = 0 \tag{18}$$

Using a Newton-Raphson approach, the following algorithm is obtained

$$[X_0^{(k+1)}] = [X_0^{(k)}] - [DF([X_0^{(k)}]) - U]^{-1} [X_T^{(k)} - X_0^{(k)}] \tag{19}$$

being **[U]** the identity matrix.

The general procedure can be summarized as follows. Starting from an initial guess of the vector of state variables $[X_0]$, a simulation is performed over one cycle to obtain $[X_T] = F([X_0])$. The periodicity constraint is checked. If it is not satisfied, the Jacobian matrix is computed and the N-R algorithm is applied. Once the vector of state variables has been updated, a time-domain simulation over a new period is performed. The procedure is continued until periodicity is achieved.

Different techniques have been developed to obtain periodic initial solution using this general procedure. They differ in the way in which the network solution (18) is formulated. Three of these techniques are summarized in this paper. The role of the state variables in all of them is played by the history current sources associated to dynamic and nonlinear branches. If a network solution is periodic, then the history current sources are also periodic, and can be used to represent the state of the discrete network as they uniquely define its solution at each time-step.

1 - Fast steady-state initialization [23]

The equations of a network containing linear and nonlinear (piecewise) components are assembled using a branch formulation and the nodal impedance matrix. A relationship between two solution vectors (the history current sources) at different time steps can be obtained. If it is formulated to obtain the values at t = T from those at t = 0, the relationship can be written as follows

$$[I_T] = [F][I_0] + [B] \tag{20}$$

being **[I]** the vector of history current sources, **[F]** a matrix which depends on dynamic elements, and **[B]** a vector related to independent sources only.

Periodicity is achieved when $[I_T] = [I_0]$, then (20) can be expressed in the following form

$$([F][I_0] + [B]) - [I_0] = 0 \qquad (21)$$

which is similar to (18). Using the N-R approach it yields

$$[I_0^{(k+1)}] = [I_0^{(k)}] - [F^{(k)} - U]^{-1}[I_T^{(k)} - I_0^{(k)}] \qquad (22)$$

This procedure is very simple and can handle unbalanced networks with nonlinear components and variable topology converters. However, **[F]** is a full matrix which is updated at every time step. These are important drawbacks for very large scale systems.

2 - The shooting method [24]

The equations of a network with nonlinear components can be expressed, using a modified nodal approach, in the following form

$$\begin{bmatrix} G & B \\ C & 0 \end{bmatrix} \begin{bmatrix} V(t) \\ I_b(t) \end{bmatrix} = \begin{bmatrix} I(t) \\ V_b(I_b(t)) \end{bmatrix} \qquad (23)$$

where **G** is the matrix of nodal conductances of the linear part, **B** and **C** are the branch incidence matrices. **V(t)** is the node voltage vector, $\mathbf{V_b(t)}$ and $\mathbf{I_b(t)}$ are the vectors of voltages and currents of the nonlinear branches. The vector $\mathbf{V_b(I_b(t))}$ denotes the functional relationship between voltages and currents in the nonlinear branches. **I(t)** is the vector of current sources, including both external current sources and history current sources, see equation (1).

If the nonlinear branches are represented by means of piecewise linear segments, the vector of branch voltages $\mathbf{V_b(t)}$ can be expressed as

$$[V_b(I_b(t))] = [R(t)][I_b(t)] + [E_k(t)] + [E_h(t) \;\; 0]^t \qquad (24)$$

where **R(t)** is a diagonal matrix of time-varying resistances, $\mathbf{E_k(t)}$ is the vector of time-varying voltages, and $\mathbf{E_h(t)}$ is the vector of Thevenin history sources.

An equivalent of the linear part of the network can be derived using the following expression

$$[V_{th}(t)] - [T][I_b(t)] = [V_b(I_b(t))] \qquad (25)$$

where $\mathbf{V_{th}(t)}$ is the vector of open circuit voltages at the nonlinear branch nodes. After joining (24) and (25), the following form is derived

$$[V_0(t)] - [E_k(t)] = [T + R(t)][I_b(t)] \qquad (26)$$

being $\mathbf{V_0(t)} = \mathbf{V_{th}(t)} - [\mathbf{E_h(t)}\ 0]^t$. Therefore a piecewise-linear N-R method can be used to solve the equations of nonlinear branches at each time step

$$[I_b^{(k+1)}(t)] = [T + R^{(k)}(t)]^{-1}[V_0(t) - E_k^{(k)}(t)] \qquad (27)$$

This solution is completely decoupled from the calculation of the unknown node voltages of the linear part of network, which can be found by solving

$$[G_{AA}][V_A(t)] = [I_A(t)] - [G_{AB}][V_B(t)] - [B_B][I_b^*(t)] \qquad (28)$$

where $\mathbf{I_b^*(t)}$ is the solution vector of the nonlinear branch currents. Equations (27) and (28) are used to perform the time-domain calculation from t=0 to t=T.

The periodic steady-state solution is obtained using the general iterative algorithm given in (19). The vector of state variables is again the vector of history current sources, which now includes sources from both linear and nonlinear elements, $[X(t)] = [I_h(t)\ \ E_h(t)]^t$.

The most complex task when applying the iterative solution (19) is the calculation of the Jacobian matrix $DF(X_0)$. This method yields a variational network with the following form

$$\begin{bmatrix} G_{AA} & B_A \\ 0 & -T - R(t) \end{bmatrix} \begin{bmatrix} V_A(t) \\ I_b(t) \end{bmatrix} = \begin{bmatrix} I_A(t) \\ E(t) \end{bmatrix} - \begin{bmatrix} G_{AB} \\ C_B \end{bmatrix} V_B(t) \qquad (29)$$

where $[E(t)] = [E_k(t)] + [E_h(t)\ \ 0]^t - [C_A][G_{AA}]^{-1}$. As shown in [24], the Jacobian $DF(X_0)$ is the solution of the sensitivity network of the variational network at time T when the initial condition is the identity matrix. In general the Jacobian $DF(X_0)$ will be a full matrix. Convergence failures have also been reported [25].

3 - The relaxation method [25]

A relationship can be found for calculating the values of the history current sources at two successive time steps

$$[X_i] = [L][X_{i-1}] - G([X_{i-1}]) \qquad (30)$$

Assume that the values of the *n* state variables are calculated in a time span T, and *m-1* solutions have been obtained from the initial estimation of the state variable vector ($i = 1$, $t = 0$) using (30). The relationship between the history current sources at two successive time steps can be written in the following form

$$F_i([X_i],[X_{i-1}]) = [X_i] - [L][X_{i-1}] - G([X_{i-1}]) = 0 \qquad (31)$$

for i = 2, ..., m. From these constraints and from the periodicity condition, $[X_1] = [X_m]$, the following N-R iterative procedure is deduced

$$\begin{bmatrix} I & 0 & 0 & \dots & 0 & -I \\ D_2 & I & 0 & \dots & 0 & 0 \\ 0 & D_3 & I & \dots & 0 & 0 \\ \dots & \dots & \dots & \dots & \dots & \dots \\ 0 & 0 & 0 & \dots & D_m & I \end{bmatrix} \begin{bmatrix} DX_1 \\ DX_2 \\ DX_3 \\ \dots \\ DX_m \end{bmatrix} = \begin{bmatrix} 0 \\ F_2 \\ F_3 \\ \dots \\ F_m \end{bmatrix} \qquad (32)$$

being $[D_i] = [dF_i/dX_{i-1}]$. The derivation of these matrices is presented in [25]. From the periodicity condition, $[F_1] = 0$. The banded form of the relaxation matrix permits the design of a very efficient algorithm.

This procedure does not require any explicit integration of the solution and it can be applied to networks with ideal diodes using a Multiple Area Thevenin Equivalent: when a diode is blocked, the related subnetworks are disconnected and solved separately.

3.3 Hybrid methods

Although most of the methods described above are very efficient, and some of them have been tested with large scale networks, no one can be applied to all potential emtp case studies. Harmonic models are not always available, and they can be specially complicated for variable topology and user-defined components; control sections are disconnected and initialized separately in most transients programs, and although some initialization features are implemented in some versions, they do not cover all capabilities. A hybrid method may benefit both frequency and time-domain methods – frequency-domain methods are used to solve the linear part for which they are more efficient, time-domain methods are used for the nonlinear and variable topology parts, see Fig. 3.

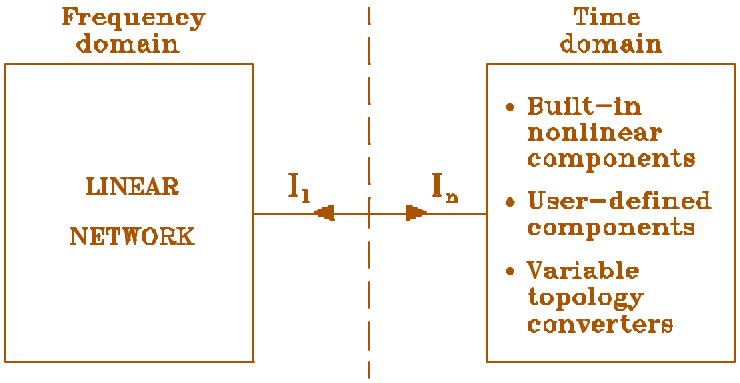

Fig. 3. Interface between linear and nonlinear parts.

The Generalized Harmonic Balance method (GHBM) presented in [26] exploits the advantages of nonlinear extrapolation methods to accelerate the computation of the periodic solution of the nonlinear parts using a time-domain calculation, while the linear part is solved using a frequency-domain calculation. Nonlinear extrapolation methods can be used to calculate the fixed solution of a vector sequence, $\mathbf{[X^{(k+1)}] = F([X^{(k)}])}$, generated using either a linear or a nonlinear process. T he Random Rank Extrapolation method was selected in [26].

The GHBM uses a two loop iterative procedure:

a) An outer loop where the periodic steady-state of the linear part is calculated using the nodal admittance equations $\mathbf{[Y_{nh}]\,[V_{nh}] = [I_{nh}]}$.

b) An inner loop where the periodic solution of the nonlinear parts is calculated using a three-step procedure:

   1. the waveforms of the voltages at the interface nodes are calculated from the harmonic phasors
   2. these voltages are used to obtain in the time-domain the steady-state waveforms of the currents injected into the nonlinear parts using a nonlinear extrapolation method
   3. the harmonic phasors of these currents are extracted. The vector of injected currents is then updated.

The whole procedure is a fixed-point iterative method. However, the nonlinear extrapolation method is also used to accelerate the convergence in the outer loop. In this manner, the method is quadratically convergent. Their advantages are obvious – no Jacobian matrix has to be calculated, and it can be applied to any case study. For a discussion about the divergence and how the problem can be solved see [26].

Other methodologies also based on a hybrid approach were presented in [27] and [28].

4. Discussion

The development of a procedure for emtp steady-state initialization that can be applied to all case studies is obviously a formidable task.

Most methods summarized in the previous sections have advantages and limitations that should be taken into account in the development of a more general and powerful procedure:

1) Frequency-domain methods are the most efficient and accurate for the calculation of the periodic steady-state of a linear network. They can handle some nonlinearities and are very adequate when the operating conditions are specified as power (load flow) constraints. The availability of harmonic models for rotating machines [18] expand their applications. However, there are many nonlinear components for which a harmonic model cannot be easily developed, and the situation becomes more complicated when a control strategy has to be included in the initialization stage.

2) Time-domain methods for emtp initialization have a very important advantage as they are fully consistent with the subsequent time-domain simulation of transients. Although the methods summarized in this paper were developed for lumped element networks, their basic ideas seem to be useful also for distributed parameter networks, but some corrective measures could be needed when many lines with different transition times are to be simulated. Numerical oscillations could be produced when a time-domain approach based on the trapezoidal rule is used, so additional corrective measures are needed, see Section 1.2 and [23]. Time domain procedures have been tested with rather simple cases, and the choice of history current sources as state variable vector could not be adequate when the system incorporates some components and control strategies.

3) Hybrid methods are an interesting alternative as they benefit from advantages of both frequency-domain and time-domain techniques. Theoretically they can handle systems incorporating all types of nonlinearities and control systems. In practice, results related to large-scale networks with frequency-dependent distributed parameter transmission lines, rotating machines and some variable-topology components have not yet been reported. And some problems remain about the convergence of the proposed techniques.

Table I shows a summary of advantages and limitations of the three classes of initialization techniques.

TABLE I - COMPARISON OF TECHNIQUES FOR EMTP INITIALIZATION

TECHNIQUE	ADVANTAGES	LIMITATIONS
Frequency-domain	• They are the most efficient for steady-state initialization of linear networks • They are also very efficient when accurate harmonic models of nonlinear components can be incorporated	• Harmonic models are not available or cannot be easily developed for some components • They cannot incorporate most control strategies
Time-domain	• The initial steady-state is consistent with the subsequent transient simulation • The choice of history current sources as state variables reduces the computational burden	• They have been applied only to simple cases • The choice of history current sources cannot be easily extended to systems with rotating machines, control strategies, user-defined components
Hybrid	• They benefit from advantages of both frequency and time domain techniques • In theory, some methods can handle all type of case studies	• They have not been tested with large scale systems which incorporate some components, i.e. rotating machines • Some convergence problems have been reported

5. Conclusions

EMTP-like programs are powerful simulation tools that can be applied in a wide range of case studies. However, their flexibility becomes an important drawback for the development of a procedure for steady-state calculation that could cover all potential cases. Many techniques have been proposed and, although no one has been yet tested in some applications, most of them can be used in many important studies. Particularly interesting are hybrid methods as they can benefit from the advantages of both frequency-domain and time-domain methods.

6. References

[1] H.W. Dommel, "Digital computer solution of electromagnetic transients in single- and multi-phase networks", *IEEE Trans. on Power Apparatus and Systems*, vol. 88, no. 2, pp. 734-741, April 1969.

[2] H.W. Dommel, EMTP Reference Manual (EMTP Theory Book), BPA, 1986.

[3] T.J. Aprille and T.N. Trick, "Steady-state analysis of nonlinear circuits with periodic inputs", *Proc. of the IEEE*, vol. 60, pp. 108-114, January 1972.

[4] D. Xia and G.T. Heydt, "Harmonic power flow studies. Part I - Formulation and solution. Part II - Implementation and practical Application", *IEEE Trans. on Power Apparatus and Systems*, vol. 101, no. 6, pp. 1257-1270, June 1982.

[5] R. Yacamini and J.C. de Oliveira, "Harmonics in multiple convertor systems : A Generalized approach", *IEE Proc.*, vol. 127, Part B, no. 2, pp. 96-106, March 1980.

[6] H.W. Dommel, "Nonlinear and time-varying elements in digital simulation of electromagnetic transients", *IEEE Trans. on Power Apparatus and Systems*, vol. 90, no. 6, pp. 2561-2567, November/December 1971.

[7] T. Noda, K. Yamamoto, N. Nagaoka and A. Ametani, "A predictor-corrector scheme for solving a nonlinear circuit", *Proceedings of IPST'97*, pp. 5-10, June 22-26, 1997, Seattle.

[8] F.L. Alvarado, R.H. Lasseter and J.J. Sanchez, "Testing of trapezoidal integration with damping for the solution of power transient studies", *IEEE Trans. on Power Apparatus and Systems*, vol. 102, no. 12, pp. 3783-3790, December 1983.

[9] P. Kuffel, K. Kent and G. Irwin, "The implementation and effectiveness of linear interpolation within digital simulation", *Electrical Power and Energy Systems*, vol. 19, no. 4, pp. 221-228, May 1997.

[10] J. Lin and J.R. Marti, "Implementation of the CDA procedure in the EMTP", *IEEE Trans. on Power Systems*, vol. 5, no. 2, pp. 394-402, May 1990.

[11] L. Dube and H.W. Dommel, "Simulation of control systems in an electromagnetic transients program with TACS", *Proc. of IEEE PICA*, pp. 266-271, 1977.

[12] R. Lasseter and J. Zhou, "TACS enhancements for the Electromagnetic Transient Program", *IEEE Trans. on Power Systems*, vol. 9, no. 2, pp. 736-742, May 1994.

[13] S. Lefebvre and J. Mahseredjian, "Improved control systems simulation in the EMTP through compensation", *IEEE Trans. on Power Delivery*, vol. 10, no. 4, pp. 1654-1662, April 1995.

[14] L. Dubé and I. Bonfanti, "MODELS : A new simulation tool in the EMTP", *European Transactions on Electrical Power Engineering*, vol. 2, no. 1, pp. 45-50, January/February 1992.

[15] H.W. Dommel, A. Yan and S. Wei, "Harmonics from transformer saturation", *IEEE Trans. on Power Systems*, vol. 1, no. 2, pp. 209-215, April 1986.

[16] W. Xu, J.R. Marti and H.W. Dommel, "A multiphase harmonic load flow solution technique", *IEEE Trans. on Power Systems*, vol. 6, no. 1, pp. 174-182, February 1991.

[17] W. Xu, J.R. Marti and H.W. Dommel, "Harmonic analysis of systems with static compensators", *IEEE Trans. on Power Systems*, vol. 6, no. 1, pp. 183-190, February 1991.

[18] W. Xu, J.R. Marti and H.W. Dommel, "A synchronous machine model for three-phase harmonic analysis and EMTP initialization", *IEEE Trans. on Power Systems*, vol. 6, no. 4, pp. 1530-1538, November 1991.

[19] J.J. Allemong, R.J. Bennon and P.W. Selent, "Multiphase power flow solutions using EMTP and Newtons method", *IEEE Trans. on Power Systems*, vol. 8, no. 4, pp. 1455-1462, November 1993.

[20] X. Lombard, J. Masheredjian, S. Lefebvre and C. Kieny, "Implementation of a new harmonic initialization method in EMTP", *IEEE Trans. on Power Delivery*, vol. 10, no. 3, pp.1343-1352, July 1995.
[21] A. Semlyen, E. Acha and J. Arrillaga, "Newton-type algorithms for the harmonic phasor analysis of non-linear power circuits in periodical steady state with special reference to magnetic non-linearities", *IEEE Trans. on Power Delivery*, vol. 3, no. 3, pp. 1090-1098, July 1988.
[22] M. Valcárcel and J.G. Mayordomo, "Harmonic power flow for unbalanced systems", *IEEE Trans. on Power Delivery*, vol. 8, no. 4, pp. 2052-2059, October 1993.
[23] J. Usaola and J.G. Mayordomo, "Fast steady-state technique for harmonic analysis", *Proc. of 4th ICHPS*, October 4-6, 1990, Budapest.
[24] B.K. Perkins, J.R. Marti and H.W. Dommel, "Nonlinear elements in the EMTP : Steady-state initialization", *IEEE Trans. on Power Systems*, vol. 10, no. 2, pp. 593-601, May 1995.
[25] Q.Wang and J.R. Marti, "A waveform relaxation technique for steady state initialization of circuits with nonlinear elements and ideal diodes", *IEEE Trans. on Power Delivery*, vol. 11, no. 3, pp. 1437-1443, July 1996.
[26] G. Murere, S. Lefebvre and X.D. Do, "A generalized harmonic balance method for EMTP initialization", *IEEE Trans. on Power Delivery*, vol. 10, no. 3, pp. 1353-1359, July 1995.
[27] A. Semlyen and A. Medina, "Computation of the periodic steady state in systems with nonlinear components using a hybrid time and frequency domain methodology", *IEEE Trans. on Power Systems*, vol. 10, no. 3, pp. 1498-1504, August 1995.
[28] J. Usaola and J.G. Mayordomo, "Multifrequency analysis with time-domain simulation", *European Transactions on Electrical Power*, vol. 6, no. 1, pp. 53-60, January/February 1996.

Load Imbalance Interharmonics in Small Adjustable Speed Drives

Mohammed Bashir Rifai
Dept. of Elect. Machines & Drives
University of Aleppo,
P. O. Box 7680, Aleppo, Syria

Thomas H. Ortmeyer
Dept. of Elect. & Computer Eng.
Clarkson University
Potsdam, NY 13699-5720 USA

Abstract The generation of low order interharmonic currents by adjustable speed drives is of concern for a number of reasons. The presence of these exciting currents at non-harmonic frequencies can excite resonances that would otherwise be dormant. Additionally, the frequency content can be close to the fundamental frequency, causing beat phenomena. The generation of these currents is reviewed here.

Introduction

The presence of interharmonic currents in adjustable speed drives (ASD's) has been the cause of some controversy. This is due to the fact that some measurements have shown these currents to be non-existent, while other measurements have found the presence of interharmonic currents.

Interharmonic currents are generally defined as steady state currents which are not an integer multiple of the fundamental frequency. In many ASD's, the input power conversion is with a diode bridge rectifier to a dc link. The dc link voltage is inverted with a PWM inverter to supply a variable frequency, variable voltage ac load. Harmonic currents of the inverter have the potential to create interharmonics in the supplying power system if they are allowed to propagate through the dc link. This paper investigates the role of load imbalance on the presence of interharmonic currents drawn from the supply system by small ASD's.

Harmonic Currents in PWM Inverters

A typical small adjustable speed drive (ASD) system is shown in Figure 1. The power source is a typical utility supply. The first power conversion is ac to dc through a single phase diode rectifier. The second conversion is a dc to ac inversion, with the inverter being pulse width modulated to construct a three phase output voltage which is of controlled frequency and magnitude.

For pwm invewrters, the harmonic currents which flow in an inverter load are related to the inverter switching frequency f_{pwm} [1] and the inverter fundamental frequency f_{inv}. Ideally, the inverter output voltage contains frequencies

$$f_{out} = nf_{pwm} \pm mf_{inv} \qquad (1)$$

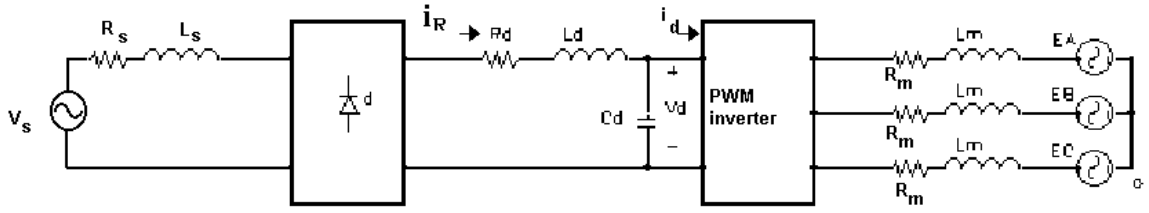

Figure 1. Simplified equivalent circuit of a typical small ASD.

with significant components limited to small integer values of m and n. Typical inverter loads have a low pass characteristic, so the current flow at these frequencies will be relatively small. The inverter switching remodulates the load fundamental frequency, so that the inverter input current will include components at a frequencies of

$$f_{in} = nf_{pwm} \pm mf_{inv} \qquad (2)$$

Again, the significant components will occur at small integer values of n and m. Currents at these frequencies will be drawn from the dc link, and can flow from the rectifier.

When the dc link choke impedance is significantly larger than the source system impedance, the dc link can be represented by the equivalent circuit shown in Figure 2. The current drawn from the rectifier will depend on the frequency of the current and the resulting impedances of the link capacitor and choke. At low frequencies, the choke will present the low impedance path for these currents, while the capacitor will be the low impedance path at high frequencies.

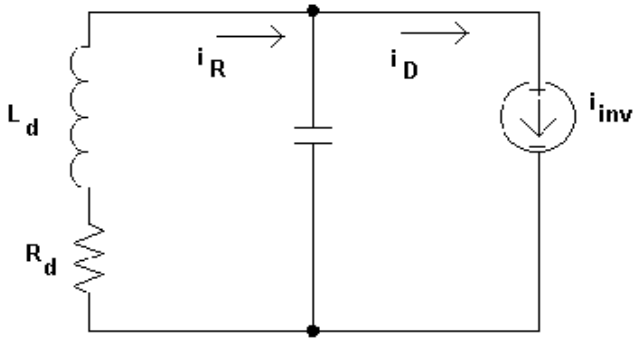

Figure 2. DC link equivalent circuit at the inverter harmonics.

As many recent inverters switch with f_{pwm} in the 5 to 20 kilohertz range, the currents drawn by the inverter due to these frequencies are high enough to be suppressed by the filtering present on the dc link.

Lower frequency currents, however, are likely to be drawn through the rectifier. Two particular cases which can lead to low frequency currents propagating through the dc link are:

- overmodulation in a sinusoidal PWM scheme
- load imbalance

Overmodulation causes lower order harmonic voltages to exist on the inverter load- typically the 5th and the 7th are most significant. These two load harmonics reflect back to the dc link as the sixth harmonic of the inverter frequency. This phenomena is relatively well understood[2]. On the other hand, load imbalance does not lead directly to harmonic currents in the load- the principal effect is a fluctuation in the instantaneous power flow. As in single phase loads, this frequency of this fluctuation is twice the inverter fundamental frequency. As the inverter neither stores nor (ideally) consumes power, the instantaneous input power closely tracks the instantaneous output power. As the inverter input voltage is nearly constant, the inverter current must include a component which is fluctuating at the second inverter harmonic. In general, this frequency will be too low to be blocked by the dc link filter.

Conversion of Inverter Harmonics into Source Interharmonics

If f_s is the source frequency and the f_{inv} is the inverter fundamental frequency, analysis of the rectifier switching shows that the source will experience interharmonic currents of frequency

$$f_{\text{int } erharmonic} = f_s \pm 2 \cdot f_{inv} \qquad (3)$$

These currents will exist due to the modulation of the rectifier output current by the rectifier switching. The input source current will also include the traditional harmonic currents drawn by the rectifier.

Laboratory Results

In order to verify the theoretical results of the previous section, laboratory measurements of a small adjustable speed drive were performed. The laboratory system employed a single phase diode rectifier feeding the dc link, with a three phase pwm inverter using the sinusiodal pwm modulation strategy. An induction motor was used for loading the inverter. The inverter was driving a 1/3 horsepower, 120/208 volt induction motor. Imbalance was created in the motor circuit by placing a rheostat in the b phase lead of the motor. The inverter was operated at 48 hertz, while the power source frequency was 60 hertz. The most significant interharmonics created by this imbalance were at 36 hertz $(2 \cdot 48 - 60)$ and at 156 hertz $(2 \cdot 48 + 60)$. Table 1 shows the relationship between these interharmonic currents and the load currents as the level of imbalance was increased.

Table 1. Load and source currents as load imbalance was increased.

Load currents, rms amps			Source currents, rms amps			
I_A	I_B	I_C	I_{60}	I_{36}	I_{156}	I_{180}
0.922	0.914	0.905	0.612	----	----	0.556
0.909	0.836	0.987	0.646	0.024	0.010	0.591
0.914	0.728	1.060	0.677	0.031	0.031	0.608
0.914	0.655	1.112	0.681	0.043	0.044	0.616
0.944	0.650	1.155	0.698	0.051	0.052	0.629

In Table 1, the load currents are the induction motor phase currents in rms amps at 48 hertz. The source currents are the frequency components of the currents going into the single phase diode bridge rectifier, with the subscript indicating the frequency of the respective currents. The data includes the 36 hertz and 156 hertz interharmonics as well as the fundamental and third harmonic components which are expected for this rectifier. As evidenced by the third harmonic current level, the dc link on this system has little if any dc link inductance.

Table 2. Relationship between load current imbalance and source interharmonic level.

Load current imbalance	Ratio of source interharmonic to fundamental
0.019	0.000
0.166	0.037
0.328	0.046
0.511	0.065
0.551	0.075

With no intentional imbalance, the interharmonic levels are negligible. As the imbalance in the phase currents increases, the interharmonic levels increase to a peak level approaching 10% of the fundamental current. While the load current imbalance for this case is extreme, the mechanism involved in the generation of the interharmonic current is apparent in these results. Table 2 shows the normalized relationship between load current imbalance and source current interharmonic level. Load current imbalance is defined as the difference between maximum and minimum phase current divided by the average phase current.

Similar performance was observed at other inverter operating frequencies, with the frequency of the interharmonic currents changing in accordance with Equation 3. The interharmonic frequency covers the full range from dc up to several multiples of operating frequency for typical ASD's. As one or more system resonance points can be expected within this range of frequnecies, it is likely that an ASD running with significantly unbalanced loading will excite a resonance at some point in it's operating range.

Conclusions

This paper analyzes the generation of source current interharmonics by inverter fed loads. The presence of inverter harmonic currents on the dc link was considered, and models were developed for the propagation of these currents through the link and onto the source system. It was shown that little if any interharmonics will be generated by well designed drives operating with linear modulation and balanced loading. Significant levels of interharmonics can be expected when low frequency inverter harmonics are present due to either load imbalance or overmodulation.

References

1. N. Mohan, T. M. Undeland and W. P. Robbins, " Power Electronics: Converters, Applications and Design", John Wiley & Sons, New York 1989.
2. David E. Rice, "A Detailed Analysis of Six-Pulse Converter Harmonic Currents", IEEE Trans. Industry Applic., vol. IA-30, no. 2, pp. 294-304, March/April 1994.

An Improved Arc Furnace Model for Digital Simulators

Omer Ozgun
ozgun@ee.tamu.edu

Ali Abur
abur@ee.tamu.edu

Department of Electrical Engineering
Texas A & M University
College Station, TX 77843 3128

Abstract - This paper describes an arc furnace model developed in the Matlab Simulink environment. The model has two characteristic features: 1) It captures the chaotic behavior of the electric arcs, 2) It generates the harmonics present in terminal current and voltage signals. The model is implemented and tested using a sample power system.

I. Introduction

Most utilities have either arc furnace loads or planning to have such loads connected to their power grid. While the bulk power consumption of arc furnaces can be predicted based on their capacity and operating cycles, instantaneous changes in power, terminal voltage and current signals are harder to calculate, particularly when the short circuit MVA at the furnace bus is relatively low. Hence, a digital model that can faithfully replicate the instantaneous behavior of an arc furnace will be useful in simulating and analyzing power system operation containing arc furnace loads.

Historically, there have been two general approaches to the problem of arc furnace modeling: stochastic and chaotic. The main reason for using stochastic ideas in modeling of arc furnaces is the a-periodic, highly varying, and unpredictable behavior of arc furnaces. In most of the previous work, in order to resemble the arc furnace voltage, modulation of arc voltage with generated white noise has been a common approach. Arc voltage has been obtained either from the simplified v-i characteristics of the arc furnace load, or from the empirical formulas related to arcing process.

However, after the electrical fluctuations in the arc furnace voltage is proved to be chaotic in nature, the deterministic chaos has become a modeling issue for electric arc furnaces [1]. In fact, chaos, also called as strange attractor, can better represent the a-periodic behavior of the arc furnaces, and seems to be closer to the nature of the process.

In this paper, a low frequency chaotic signal is obtained from Chua's well-known chaotic circuit and modulated with the arc voltage to represent the electrical fluctuations in the arc furnace voltage. On the other hand, arc voltage is simulated by solving the corresponding differential equation which yields a dynamic and multi-valued v-i characteristics of the arc furnace load. The proposed arc furnace model takes the system current as an input and assigns the terminal voltage value at each time step. Namely, it is connected to the system as a controlled voltage source.

II. Proposed Arc Furnace Model

The proposed model is composed of two main parts:

- The use of dynamic, multi-valued voltage-current characteristics of the electric arc.
- A chaotic circuit is used to represent the arc furnace voltage fluctuations, which are chaotic in nature.

Dynamic Behavior of Electric Arcs

The dynamic v-i characteristics of arc furnace load is obtained by using a general dynamic arc model in the form of a differential equation derived in [2]. Thanks to development of a general dynamic arc model, a non-linear, multi-valued, and dynamic voltage-current characteristics of arc furnace load is captured. This makes a fundamental difference between this approach and the others where the electric arc is represented by its static v-i characteristics or some empirical relations. Having a dynamic arc model makes the arc furnace model more reliable, since it will capture changes in the v-i characteristics as the operating conditions change in the power system.

The differential equation that represents the general dynamics of the arc model is based on the principle of energy conversion. Therefore, starting from the power balance equation for the electric arc, the following differential equation is derived in [2]:

$$k_1 r^n + k_2 r \frac{dr}{dt} = \frac{k_3}{r^{m+2}} i^2 \qquad (1)$$

Here "r", which stands for the arc radius, is chosen as a state variable instead of taking arc resistance or conductance. While solving equation 1, the parameters are chosen as k_1=3000, k_2=1, and k_3=12.5. And the arc voltage is then given by:

$$v = \frac{i}{g} \qquad (2)$$

where g is defined as arc conductance and given by the following equation:

$$g = \frac{r^{m+2}}{k_3} \qquad (3)$$

Figure 1 shows the dynamic v-i characteristics of 250 V, 70-kA a.c. electric arc obtained by solving equations 1 and 2 in time domain. The simulated v-i characteristics of electric arc matches well with the measured characteristics [2]. The simulated arc voltage waveform is shown in Figure 2.

Chaotic Time Variation

The chaotic component of the arc furnace voltage is supplied from the well known chaotic circuit of Chua [3, 4].

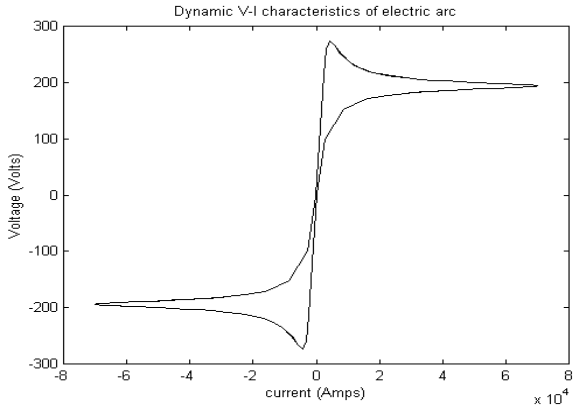

Figure 1. Dynamic v-i characteristics of electric arc

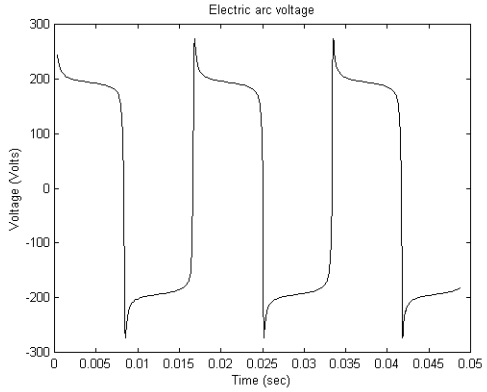

Figure 2. Typical voltage waveform of electric arc.

Arc Furnace Model

The model is built and simulations are carried out in Matlab-Simulink environment. The deterministic part of the model, namely representation of dynamic v-i characteristics of electric arc solving the differential equation of equation 1, is implemented by using ordinary Simulink blocks. However, the simulation of Chua's chaotic circuit is performed by using the new Power System Blockset of Matlab. More detailed information about the proposed arc furnace model can be found in [5], which will be published in the proceedings of the IEEE Power Engineering Society 1999 summer meeting.

Two voltage signals, one obtained from the simultaneous solution of the corresponding differential equation of the electric arc, and the other obtained from the simulation of Chua's chaotic circuit, are the basic components of the final output voltage of the arc furnace model, which is basically equal to the modulation of those two signals. The input to the model is the current absorbed from the power system bus.

III. Simulation Results

The proposed model is tested by using a sample power system, which consists of linear loads and an electric arc furnace load connected to the secondary of the step-down transformer. Figure 3 shows the current waveform obtained by simulation. The flicker effect can easily be observed in this simulated waveform.

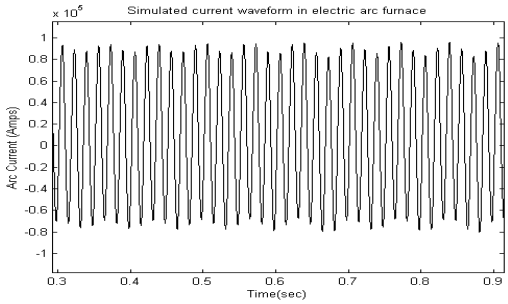

Figure 3. Arc Current obtained by simulation

Figure 4 shows the voltage waveform at secondary of the transformer

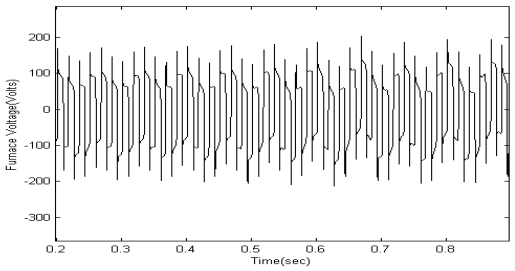

Figure 4. Voltage at secondary of the arc furnace transformer

For an accurate arc furnace model, capturing the harmonic spectrum of the arc furnace current and voltages is also a very important criterion, as well as capturing the flicker effect. Although the previous models are able to capture the odd harmonics, they have difficulty in capturing the even ones. Figure 5 shows the harmonic spectrum of the simulated voltage waveform. As it is seen, even harmonics are captured by the proposed model as well. Additionally, the magnitudes of the harmonics change from cycle to cycle during the simulation, and Figure 5 shows a single snapshot during the simulation period.

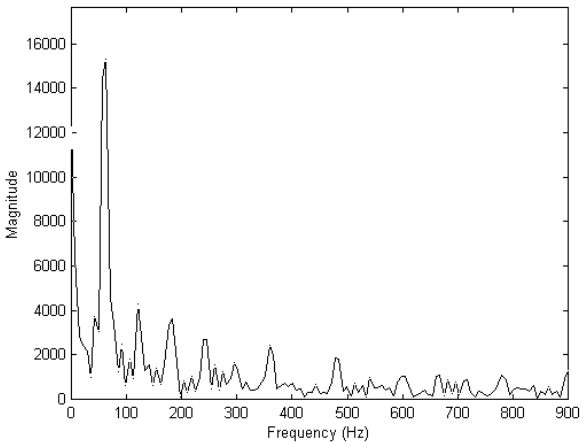

Figure 5. Harmonic analysis of simulated voltage waveform

IV. Conclusions

This paper introduces a new model to represent the arc furnace operation in an accurate way. The model is built in the time domain and it can be readily connected at a specified bus as a circuit component, which takes the system current as input and assigns the terminal voltage value at each time step, i.e., it behaves like a controlled voltage source.

Instead of using static v-i characteristics of the arc furnace load, dynamic and multi-valued v-i characteristics are obtained by solving the corresponding differential equation. In order to represent the flicker effect, a low frequency chaotic signal is modulated with the arc voltage. So, the symmetry of the arc v-i characteristics is destroyed, resulting in the even harmonics as well as the odd ones.

V. Acknowledgements

The authors gratefully acknowledge the support provided by the Texas Higher Education and Coordination Board Advanced Technology Program Grant No: 000512-0094-1997.

References

1. E. O'Neill-Carrillo, G. Heydt, E. J. Kostelich, S. S. Venkata, A. Sundaram, "Nonlinear Deterministic Modeling of Highly Varying Loads," IEEE Transactions on Power Delivery, July 1998.
2. E. Acha, A. Semlyen, N. Rajakovic, "A Harmonic domain Computational Package for Nonlinear problems and Its Application to Electric Arcs," IEEE Transactions on Power Delivery, vol. 5, no. 3, July. 1990, pp. 1390-1397.
3. M. P. Kennedy, "Three Steps to Chaos, Part 1:Evolution," IEEE Transactions on Circuit and Systems-I: Fundamental Theory and Applications, Vol. 40, No. 10, October 1993, pp.640-656.
4. M. P. Kennedy, "Three Steps to Chaos, Part 2:A Chua's Circuit Primer," IEEE Transactions on Circuit and Systems-I: Fundamental Theory and Applications, Vol. 40, No. 10, October 1993, pp.657-674.
5. O. Ozgun, A. Abur, "Development of an Arc Furnace Model for Power Quality Studies," IEEE PES '99 Summer Meeting proceedings, July 18-22, 1999, Edmonton, Alberta, Canada.